

## Interplay between structural randomness, composite disorder, and electrical response: Resonances and transient delays in complex impedance networks

R. Huang, G. Korniss,\* and S. K. Nayak

*Department of Physics, Applied Physics, and Astronomy, Rensselaer Polytechnic Institute, 110 8th Street, Troy, New York 12180-3590, USA*

(Received 2 March 2009; revised manuscript received 26 August 2009; published 1 October 2009)

We study the interplay between structural and conductivity (composite) disorder and the collective electrical response in random network models. Translating the problem of time-dependent electrical response (resonance and transient relaxation) in binary random composite networks to the framework of generalized eigenvalues, we study and analyze the scaling behavior of the density of resonances in these structures. We found that by controlling the density of shortcuts (topological randomness) and/or the composite ratio of the binary links (conductivity disorder), one can effectively shape resonance landscapes or suppress or enhance long transient delays in the corresponding random impedance networks.

DOI: [10.1103/PhysRevE.80.045101](https://doi.org/10.1103/PhysRevE.80.045101)

PACS number(s): 89.75.Hc, 84.30.Bv, 05.60.Cd

Resistor networks have been widely studied since the 1970s as models for conductivity problems and classical transport in disordered media [1]. With the recent surge of research on complex networks [2], resistor networks and related flow models have been employed to study and explore community structures in social networks [3] and to construct recommendation models for community networks [4]. Also, resistor networks, as abstract models for network flows with a fundamental conservation law [5], were utilized to study transport in complex networks [6–11].

Complex impedance networks have been investigated to study electrical and optical properties of two-dimensional thin films [12,13] and dielectric resonances of two-dimensional regular lattice structures, lattice animals, and other fractal clusters [14–17]. In this Rapid Communication, we investigate electrical response (resonances and delays) when *both* the structure and the composition of the local conductances can be random, and we focus on the interplay between structural and composite disorders and response. Random structures, with links being effective circuit elements to model current flow, are ubiquitous in complex materials [18–22] and biological systems [23–25]. For example, in a random nanowire network made of single-wall carbon nanotubes, the individual wires can be either conductors or semiconductors (based on their individual chiralities), resulting in links with (binary) composite disorder; their natural composition comes with a dominance of the semiconducting tubes [21]. In turn, studying fundamental complex conductivity problems in these networks will help one understand the time-dependent intrinsic electrical response (resonances and transient delays) of these devices which have to switch electric currents on and off and driven by high clock speeds. Likewise, inherent delays in electrical signal propagation can have crucial effects on processes in neuronal networks [24]. For example, the compartmental-model representation of passive dendritic trees is an  $R_1C$ - $R_2$  network (each compartment consists of an  $R_1$  membrane leakage resistor in parallel with a capacitance  $C$  and compartments are connected with

an  $R_2$  junctional resistor) [25]. The framework employed here can be employed to study the effects of local defects (damaged or destroyed links) on global signal delays ultimately governed by the structure and link disorder in the network.

The networks in the above examples are embedded in (multilayer) two-dimensional (nanowire network) and three-dimensional space (neuronal network). As a result of topological constraints and “wiring-cost” considerations [23,26]), only a small fraction of links are long ranged. The common features of the underlying network topologies is that they are spatially embedded, random, sparse, and the presence of long-range links are strongly suppressed. Here, we investigate the fundamental aspects of the interplay between topological randomness, conductivity disorder, and system response, precisely for these network structures.

While the resonance and relaxation properties are well understood in low-dimensional structures with conductivity (bond) disorder [16], and recently on the complete graph [27], to our knowledge, a similar investigation on complex random network structures with link conductivity disorder has not been performed. We employ the framework applicable to binary link disorder [12,15,16,27]. The powerful feature of the framework is that it can be employed to study the singularities of the electrical response associated with any kind of binary link disorder on any graph (random  $L$ - $C$ ,  $RL$ - $C$ ,  $R$ - $C$ , or more complicated composite circuits, involving two but individually arbitrarily complicated building blocks).

The equations governing current flows in any network can be written as [5,10,17]  $\sum_j \sigma_{ij}(V_i - V_j) = I(\delta_{is} - \delta_{it})$ , where  $\sigma_{ij}$  are now the possibly complex link conductances. Nodes  $s$  and  $t$  are the nodes where a current  $I$  enters and leaves the network, respectively. The above equation can be rewritten as  $\sum_j L_{ij}V_j = I(\delta_{is} - \delta_{it})$ , where  $L_{ij} = \delta_{ij}\sum_{l \neq i} \sigma_{il} - \sigma_{ij}$  is the Laplacian of the underlying graph with complex couplings also referred to as the admittance matrix in the present context.

For example, in  $L$ - $C$  composite networks (or in  $RL$ - $C$  composite networks with weak dissipation), in order to find resonance frequencies one can identify the nontrivial singularities, the “zeros” of the admittance matrix (corresponding

\*Corresponding author. [korniss@rpi.edu](mailto:korniss@rpi.edu)

to the “poles” of the complex impedance matrix), i.e., requiring that zero input current gives rise to finite potential differences in the network [16,17]. One can also show that the zeros of the conductivity matrix are directly related to the transient relaxation times in  $R$ - $C$  composite networks, characterizing how fast the system responds to steplike on/off signals [15,16]. For binary composite networks, the conductance disorder of existing links in the structure is characterized by a single parameter (composite ratio)  $q$ , such that  $\sigma_{ij}=\sigma_1$  with probability  $q$ , and  $\sigma_{ij}=\sigma_2$  with probability  $(1-q)$  (and obviously,  $\sigma_{ij}=0$  if nodes  $i$  and  $j$  are not connected). For example, for an  $L$ - $C$  composite network,  $\sigma_1=i\omega C$ ,  $\sigma_2=(i\omega L)^{-1}$ , while for an  $R$ - $C$  composite network,  $\sigma_1=i\omega C$ ,  $\sigma_2=R^{-1}$ . Hence, for resonance condition in  $L$ - $C$  networks (and for relaxation times for  $R$ - $C$  networks), one searches for the nontrivial solutions of  $\sum_j L_{ij}(\omega)V_j=0$  or  $\mathbf{L}(\omega)\mathbf{V}=\mathbf{0}$  in a more compact notation. Then for any fixed graph and any realization of the binary link disorder, one can rewrite the above expression for the resonance condition (or to extract transient relaxation times) [27],

$$(\mathbf{H}-\lambda\mathbf{\Gamma})\mathbf{V}=\mathbf{0}, \quad \lambda=(\sigma_1+\sigma_2)/(\sigma_1-\sigma_2). \quad (1)$$

Here,  $H_{ij}=\delta_{ij}\sum_{l\neq i}h_{il}-h_{ij}$ , where  $h_{ij}=-1, +1, 0$  if  $\sigma_{ij}=\sigma_1, \sigma_2, 0$ , respectively. Similarly,  $\Gamma_{ij}=\delta_{ij}\sum_{l\neq i}e_{il}-e_{ij}$ , is just the (topological) network Laplacian of the underlying graph, where  $e_{ij}=|h_{ij}|=1, 0$  is the network adjacency matrix [28]. The expression for  $\lambda$  in Eq. (1) establishes the connection between the generalized eigenvalues and the resonance frequencies  $\omega_j$  of  $LC$  [29] or the transient relaxation times  $\tau_j$  of  $RC$  composite networks [30],

$$\omega_j=(1/\sqrt{LC})\sqrt{(1+\lambda_j)/(1-\lambda_j)}, \quad \tau_j=RC(1-\lambda_j)/(1+\lambda_j). \quad (2)$$

Hence the above generalized eigenvalue problem Eq. (1), where  $\mathbf{\Gamma}$  is real symmetric and non-negative and  $\mathbf{H}$  is real symmetric, provides a framework to identify the resonance frequencies (density of resonances in the large  $N$  limit) or relaxation times in the respective binary composite networks. It is also clear from the above framework that the resonance (and relaxation) spectrum (except from pathological cases) is *independent* of the choice of nodes where the current enters and leaves the system, thus, they represent *intrinsic characteristics* of the network [15–17].

In what follows, for brevity, we use the “resonance” terminology in composite networks and will also refer to  $\lambda$  as “frequency.” The eigenvalues of the above system always fall in the  $[-1, +1]$  interval,  $\lambda_1\leq\lambda_2\leq\cdots\leq\lambda_N$ , with “true” resonances corresponding to  $-1<\lambda_j<1$  ( $0<\omega_j<\infty$ ) [31]. We focused on two important observables, the density of resonances  $\rho(\lambda)$  and number of resonances *per node*  $\bar{\rho}$  [15,16,27]

$$\rho(\lambda)=\frac{1}{N}\sum_{\alpha=1}^{n_R}\delta(\lambda-\lambda_\alpha), \quad \bar{\rho}=\int\rho(\lambda)d\lambda=\frac{n_R}{N}, \quad (3)$$

where  $n_R$  is the total number of true resonances (not associated with  $\lambda_j=\pm 1$ ). In this work, we determined the spectrum of the generalized eigenvalue problem Eq. (1) numerically and constructed the above observables by averaging over

10 000 realizations (1000 realizations for the largest system size) of both structural and composite disorders.

Before studying random structures with binary composite disorder, we recall two known extreme cases: the one-dimensional (1D) ring and the complete graph, both with the same composite (binary link) disorder. For a one-dimensional ring, there is a single resonance frequency [17] (which can also be obtained via elementary considerations). More specifically,  $n_R=1$  and the frequency is distributed binomially about  $\langle\lambda\rangle=2q-1$ . Thus, in the large- $N$  limit, the density of resonances [Eq. (3)] approaches a Gaussian distribution with the above mean and vanishing width, i.e., a delta function. For example, for  $q=1/2$ ,  $\rho(\lambda)\simeq\frac{1}{N}\delta(\lambda)$  and  $\bar{\rho}=\frac{1}{N}$ .

In the other extreme case where all nodes are connected to all others (i.e., the complete graph), using a path-integral approach [27,32] in the large- $N$  limit, it was obtained (with-

out loss of generality, for  $q=1/2$ ) that  $\rho(\lambda)\xrightarrow{N\rightarrow\infty}\delta(\lambda)$  and  $\bar{\rho}\xrightarrow{N\rightarrow\infty}1$ , i.e., the total number of resonances approaches the number of nodes, but they are all narrowly centered about the same frequency (becoming fully degenerate as  $N\rightarrow\infty$ ).

Now, we consider small-world (SW) networks [33] as random structures, where random shortcuts were *added* to a one-dimensional ring (1D SW) [10,34], resulting in an average number of random shortcuts per node  $p$ . For comparison with the previous two extreme cases, we show results for the same composite ratio  $q=1/2$ . The results show that for any nonzero value of  $p$ , the number of resonances per node will approach a nonzero  $\bar{\rho}>0$  value in the large- $N$  limit as opposed to the pure 1D ring where it vanishes as  $1/N$  [Fig. 1(a)]. Further, as the number of random links per node  $p$  increases,  $\bar{\rho}$  increases monotonically, and the density of resonances initially [ $0<p\leq O(1)$ ] widens; at around  $p\sim O(1)$ , the spectrum becomes *extended* [Fig. 1(b)].

As we further increase  $p$ , the number of resonances per node continues to increase monotonically as a function  $p$ , quickly “saturating” to its maximum value  $\bar{\rho}=1$  [Fig. 1(a)], while the density of resonances becomes progressively centered about  $\lambda=0$  [Figs. 1(b) and 1(c)], eventually converging to a delta-function (if both  $p\rightarrow\infty$ ,  $N\rightarrow\infty$ ). Indeed, one can recall for the complete graph that the average number of resonance per node approaches  $\bar{\rho}=1$ , but all frequencies are centered about the same value [27]. Note that in both the low shortcut density [ $0<p\ll O(1)$ , Figs. 2(a) and 2(b)] and the high shortcut density [ $p\gg O(1)$  (not shown)] regimes, for fixed  $p$ , the density of resonances becomes independent of the size of the network for large  $N$ . Finite-size effects are very strong, however, for  $p\sim O(1)$ , in particular in the low- and high-frequency regimes Fig. 2(c)]. Further analysis in the high-connectivity [ $p\gg O(1)$ ] regime also reveals that the limit density of resonances has the scaling form  $\rho(\lambda)=p^{1/2}\phi(p^{1/2}\lambda)$  [Fig. 1(c) and inset]. This scaling form, valid for all  $p\gg O(1)$ , is identical to the one found for regular long-range connectivity graphs [32], including the limit of complete graph ( $p\rightarrow N$ ) [35].

Next, we provide more details for the low shortcut-density regime (also referred to as the SW regime),  $0<p\ll O(1)$ . The scaling of the number of resonances per node  $\bar{\rho}$  in this regime [Fig. 1(a)] can be extracted from the finite-size

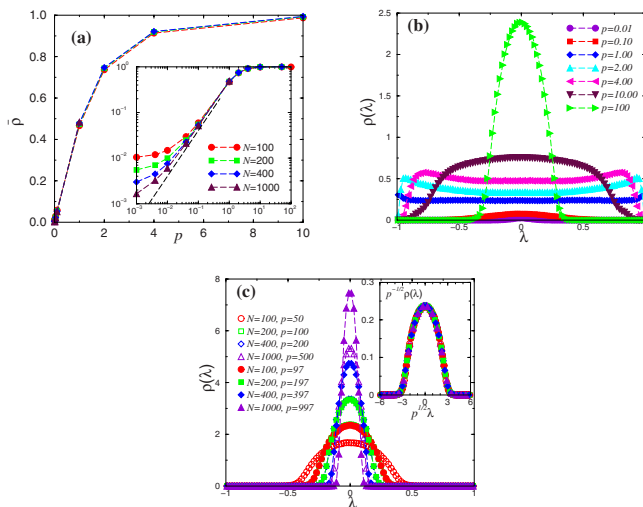


FIG. 1. (Color online) (a) Average number of resonances per node vs density of shortcuts  $p$  in a 1D SW network with composite ratio  $q=1/2$ . The inset shows the same data on log-log scales, with the straight dashed line indicating the asymptotic large- $N$  behavior,  $\bar{\rho} \sim p$ . (b) Density of resonances for fixed number of nodes  $N=1000$  with  $q=1/2$ , and for different values of  $p$ . (c) Density of resonances in the large- $p$  regime for  $q=1/2$  for various system sizes. The inset shows the scaled plot of the same data,  $\rho(\lambda)/p^{1/2}$  vs  $p^{1/2}\lambda$ . These and the following plots all show ensemble averages over 10 000 network- and composite-disorder realizations (1000 for the largest system size).

behavior, typical in 1D SW networks [10,34]. Since the number of random links per node (density of shortcuts) is  $p$ , the typical (Euclidean) distance between nodes with shortcuts emanating from them scales as  $\xi \sim p^{-1}$ . Thus, for  $N \ll \xi$  ( $Np \ll 1$ ), there are no random links in almost any realization

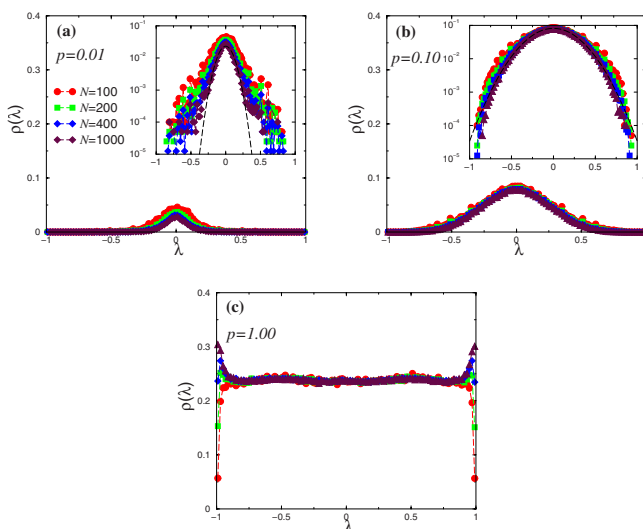


FIG. 2. (Color online) Density of resonances in 1D SW networks for different system sizes for composite ratio  $q=1/2$  and for (a)  $p=0.01$ , (b)  $p=0.10$ , and (c)  $p=1.00$ . System sizes and the corresponding symbols in all three panels are the same as in (a). The insets in (a) and (b) show the same data on lin-log scales and a Gaussian fit to the largest system size around the center (dashed curve).

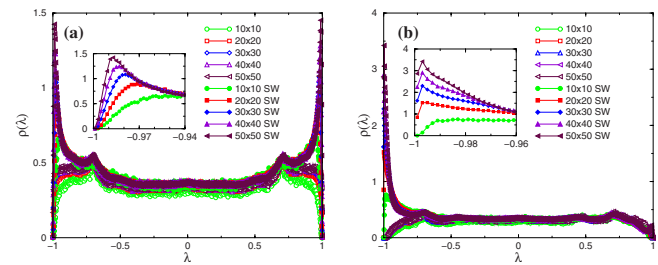


FIG. 3. (Color online) (a) Density of resonances in regular 2D ( $p=0$ , open symbols) and power-law-suppressed 2D SW networks ( $p=1.00$ ,  $\alpha=1.00$ , solid symbols) for different system sizes ( $N=L \times L$ ), and for composite ratio  $q=1/2$ . The insets show the same data enlarged for the 2D SW network in the vicinity of one of the peaks. (b) The same plot as (a) for composite ratio  $q=2/3$ .

of the network, and the resonance structure will essentially be identical to that of the pure ring. A crossover governed by the emerging SW structure can be expected when  $N \gg \xi$  ( $Np \gg 1$ ). Thus, in the SW regime,  $0 < p \ll O(1)$ , for arbitrary  $N$ , the above crossover behavior of  $\bar{\rho}(N, p)$  can be expressed in terms of  $N$  and the scaled variable  $x = Np$  with the help of a scaling function  $f(x)$ , such that

$$\bar{\rho}(N, p) = (1/N)f(Np), \quad (4)$$

where  $f(x) \sim \text{const}$  for  $x \ll 1$ , while  $f(x) \sim x$  for  $x \gg 1$ . Thus, in the large network-size limit ( $N \rightarrow \infty$ ), for *small* values of  $p$ ,  $\bar{\rho} \sim p$ , i.e., the number of resonance per node increases linearly with the average number of random links per node as can be seen in Fig. 1(a) (inset). Our numerical results also suggest (although with considerable finite-size effects for finite networks) that for any *fixed*  $0 < p \ll 1$  value,  $\rho(\lambda)$  approaches a system-size-independent limit density and obeys the scaling form  $\rho(\lambda) \sim \bar{\rho}(p)p^{-1/2}\Psi(\lambda/p^{1/2}) \sim p^{1/2}\Psi(\lambda/p^{1/2})$ . Further, the scaling function  $\Psi(s)$  is reasonably well approximated by  $\sim e^{-cs^2}$  in the vicinity of the center as  $N \rightarrow \infty$ , i.e., the density of resonances approaches a Gaussian shape [Figs. 2(a) and 2(b)].

Finally, to model spatially embedded random structures with topological constraints [26,36], we considered when *both* the value of the complex link conductivity and the probability to have a link between two nodes can depend on Euclidean distance between the two nodes it connects. From elementary length scale considerations, for the distance-dependent link conductivity, one has  $\sigma_{ij} \sim 1/d_{ij}$ , where  $d_{ij}$  is the Euclidean distance between nodes  $i$  and  $j$  (assuming uniform “wire” cross sections) [Eq. (1) easily generalizes to this case.] Whereas the probability of having a link (shortcut) between node  $i$  and  $j$ , can also be suppressed, e.g.,  $p_{ij} \sim 1/d_{ij}^\alpha$  (power-law-suppressed SW networks due to wiring-cost considerations or topological constraints [26,36]).

In Fig. 3(a), we show the resonance spectrum of a *two-dimensional* power-law-suppressed SW network (2D SW) with open boundaries with  $\alpha=1$  and  $p=1.00$  (random shortcuts with distance-dependent conductivities were *added* on top of a two-dimensional regular “substrate,” with composite ratio  $q=1/2$ , together with the known results [14,16] of the regular two-dimensional topological structures with the same

composite disorder. For regular two-dimensional structures, in the large-system size limit,  $\bar{\rho} \sim O(1)$  and the spectrum is known to be *extended* [14,16]. The addition of distance-dependent shortcuts, however, strongly modifies the density of resonances in the vicinity of  $\lambda \approx \pm 1$  (strong peaks for low and high frequencies). Further, the structure of the peaks does not approach a limit density in that region but diverges with system size (with  $p$  fixed). An analogous plot for an asymmetric link disorder with  $q=2/3$  [Fig. 3(b)] shows strong (diverging) peaks only in the small-frequency regime [also translating to large transient relaxation times or delays in RC networks Eq. (2)]. Our analyses also indicate that the main qualitative features (articulated peaks for low and/or high frequencies) of structures with distance-dependent shortcuts prevail for a range of  $\alpha$ ,  $0 \leq \alpha \leq \alpha_c \approx 2 \pm 0.5$ .

In summary, we have shown that in random composite

networks by controlling the density of shortcuts  $p$  (topological randomness) and/or the composite ratio  $q$  of the binary links (conductivity disorder), one can effectively shape the resonance landscape or suppress or enhance long transient delays in electrical signal propagation. Here, we have highlighted the fundamental aspects of the interplay between structural and composite (conductivity) disorders and the collective electrical response in spatially embedded sparse random networks models. The electrical response of more realistic off-lattice spatially embedded random structures, reflecting relevant wiring cost and topological constraints [19,26] will be considered in future works.

This work was supported in part by NSF Grant No. DMR-0426488 and DTRA Award No. HDTRA1-09-1-0049. R.H. and S.K.N were also supported in part by the Focus Center, NY at RPI.

- 
- [1] S. Kirkpatrick, Rev. Mod. Phys. **45**, 574 (1973).  
 [2] R. Albert and A.-L. Barabási, Rev. Mod. Phys. **74**, 47 (2002).  
 [3] M. E. J. Newman and M. Girvan, Phys. Rev. E **69**, 026113 (2004).  
 [4] Y.-C. Zhang *et al.*, Phys. Rev. Lett. **99**, 154301 (2007).  
 [5] F. Y. Wu, J. Phys. A **37**, 6653 (2004).  
 [6] G. Korniss, Phys. Rev. E **75**, 051121 (2007).  
 [7] J. S. Andrade *et al.*, Phys. Rev. Lett. **94**, 018702 (2005).  
 [8] E. López *et al.*, Phys. Rev. Lett. **94**, 248701 (2005).  
 [9] L. K. Gallos *et al.*, Proc. Natl. Acad. Sci. U.S.A. **104**, 7746 (2007).  
 [10] G. Korniss *et al.*, Phys. Lett. A **350**, 324 (2006).  
 [11] T. Antal and P. L. Krapivsky, Phys. Rev. E **74**, 051110 (2006).  
 [12] J. P. Straley, J. Phys. C **12**, 2143 (1979).  
 [13] X. Zhang and D. Stroud, Phys. Rev. B **52**, 2131 (1995).  
 [14] J. P. Clerc *et al.*, J. Phys. A **29**, 4781 (1996).  
 [15] J. P. Clerc *et al.*, Adv. Phys. **39**, 191 (1990).  
 [16] Th. Jonckheere and M. Luck, J. Phys. A **31**, 3687 (1998).  
 [17] W. J. Tzeng and F. Y. Wu, J. Phys. A **39**, 8579 (2006).  
 [18] J. A. Davis *et al.*, IEEE Trans. Electron Devices **45**, 580 (1998).  
 [19] C. Teuscher, Chaos **17**, 026106 (2007).  
 [20] Q. Cao *et al.*, Nature (London) **454**, 495 (2008).  
 [21] G. Gruner, J. Mater. Chem. **16**, 3533 (2006).  
 [22] A. F. Holloway *et al.*, J. Phys. Chem. C **112**, 13729 (2008).  
 [23] S. B. Laughlin and T. J. Sejnowski, Science **301**, 1870 (2003).  
 [24] O. Sporns and J. D. Zwi, Neuroinformatics **2**, 145 (2004).  
 [25] C. Koch, *Biophysics of Computation* (Oxford University Press, New York, 1999).  
 [26] T. Petermann and P. De Los Rios, Phys. Rev. E **73**, 026114 (2006).  
 [27] Y. V. Fyodorov, J. Phys. A **32**, 7429 (1999); Physica E **9**, 609 (2001).  
 [28] Equation (1) follows from the identity [27]  $\sigma_{ij}=1/2[(\sigma_1+\sigma_2)e_{ij}-(\sigma_1-\sigma_2)h_{ij}]=(\sigma_1-\sigma_2)/2[(\sigma_1+\sigma_2)/(\sigma_1-\sigma_2)e_{ij}-h_{ij}]$ , where  $e_{ij}=1,0$  is the network adjacency matrix and  $h_{ij}=-1,+1,0$  if  $\sigma_{ij}=\sigma_1, \sigma_2, 0$ , respectively. Hence, the admittance matrix can be written as  $\mathbf{L}=(\sigma_2-\sigma_1)/2(\mathbf{H}-\lambda\mathbf{I})$ .  
 [29] Solving the generalized eigenvalue problem,  $\mathbf{H}\mathbf{u}_l=\lambda_l\mathbf{I}\mathbf{u}_l$  (with normalization  $\mathbf{u}_k\mathbf{I}\mathbf{u}_l=\delta_{kl}$ ), one can formally express the voltage differences between any pairs of nodes employing their spectral decomposition. In particular, for an ac current with amplitude  $I$  entering (leaving) the network at node  $s(t)$ , respectively, the frequency-dependent voltage amplitude between these two nodes can be expressed as  $V(\lambda)=V_s-V_t=2I/(\sigma_2-\sigma_1)\sum_l(u_{ls}-u_{lt})^2/(\lambda_l-\lambda)$ .  
 [30] Considering a step-function signal  $I(t)=I_0\theta(t)$  running through the network, and employing  $V(\lambda)$  from [29] as the solution in Fourier space, the voltage response can be expressed as  $V(t)=\int_{-\infty}^{\infty}d\omega/2\pi e^{i\omega t}/(i\omega+0)2I_0/(\sigma_2-\sigma_1)\sum_l(u_{ls}-u_{lt})^2/(\lambda_l-\lambda)$ . For the *transient* part of the voltage, one obtains  $V^{\text{trans}}(t)=\sum_{\alpha=1}^{n_R}c_\alpha e^{-t/RC(1+\lambda_\alpha)/(1-\lambda_\alpha)}$ , where the sum runs over only the  $\lambda_\alpha \neq \pm 1$  solutions, and the  $c_\alpha$  coefficients can be expressed in terms of the corresponding eigenvalues and eigenvectors.  
 [31] For example, in LC networks, the number of solutions with  $\lambda_j=-1,1$  ( $\omega_j=0,\infty$ ) corresponds to the number of purely L or C clusters in the network, respectively [16].  
 [32] J. Ståring *et al.*, Phys. Rev. E **67**, 047101 (2003).  
 [33] D. J. Watts and S. H. Strogatz, Nature (London) **393**, 440 (1998).  
 [34] M. E. J. Newman and D. J. Watts, Phys. Lett. A **263**, 341 (1999).  
 [35] While the shape of the scaling function  $\phi(u)$  is nontrivial, its tail asymptotically decays as  $\phi(u) \sim e^{-u^2/2}$  [27].  
 [36] B. Kozma *et al.*, Phys. Rev. Lett. **95**, 018701 (2005).